Dual-Modal Nanoplasmonic Light Upconversion in Broadband Multiresonant Plasmonic Metasurfaces

Seied Ali Safiabadi Tali, and Wei Zhou*

Department of Electrical and Computer Engineering, Virginia Tech, Blacksburg, Virginia 24061, United States
**Email: wzh@vt.edu*

Abstract: This study investigates dual-modal plasmon-enhanced light upconversion, combining anti-Stokes photoluminescence (ASPL) and second-harmonic generation (SHG) in $Ag/SiO_2/Ag$ nanolaminate plasmonic crystal metasurfaces. It highlights the distinct emission behaviors of ASPL and SHG in multiresonant plasmonic nanocavities. © 2024 The Author(s)

OCIS codes: (350.4238) Nanophotonics and photonic crystals; (250.5403) Plasmonics; (240.6680) Surface plasmons.

1. Summary

The pursuit of efficient light upconversion in nanostructures has significant implications for applications ranging from bioimaging and sensing to photonics[1, 2]. Our research[3] focuses on dual-modal nanoplasmonic light upconversion, integrating anti-Stokes photoluminescence (ASPL) and second-harmonic generation (SHG) within the same broadband multiresonant metal nanocavities (**Fig. 1**). This integration in two-tier $Ag/SiO_2/Ag$ nanolaminate plasmonic crystal (NLPC) metasurfaces addresses the challenge of achieving multiresonant enhancement for both ASPL and SHG, a prerequisite for applications relying on dual-modal or wavelength-multiplexed operations.

Our approach encompasses both experimental and theoretical aspects. We utilize NLPC metasurfaces (**Fig. 1**) capable of supporting multiple hybridized plasmon modes with significant spatial mode overlaps[3]. This configuration enhances multiphoton excitation and emission transitions for both ASPL and SHG. Our experiments (**Fig. 2**) probe the distinctions and correlations between ASPL and SHG processes under various ultrashort pulsed laser excitation conditions, including incident fluence, wavelength, and polarization. Complementing these measurements, we developed a time-domain modeling framework (**Fig. 3**) to analyze the observed effects and to understand the intricate dynamics of mode coupling enhancement, quantum transitions, and hot carrier population mechanics. Our findings reveal that ASPL and SHG while coexisting in the same metal nanocavities, exhibit markedly different plasmon-enhanced emission behaviors. Incoherent hot carriers mediate the ASPL process with temporally evolving energy and spatial distributions. In contrast, SHG emissions are instantaneous. We also demonstrate that NLPC metasurfaces support multiple hybridized plasmons, facilitating the broadband multiresonant enhancement essential for ASPL and SHG upconversion processes. These insights contribute significantly to understanding the complex interplay between different plasmonic emissions and the conditions affecting them.

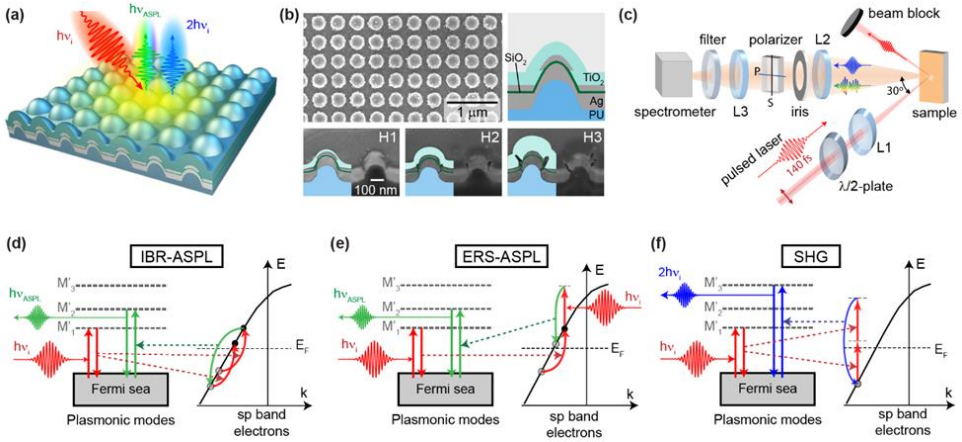

Figure 1: Examining SHG and ASPL in NLPC metasurfaces. (a) Illustration of SHG and ASPL emissions from NLPC under NIR ultrashort pulsed laser excitation. (b) Top-view and cross-sectional SEM images of NLPC with varying TiO_2 capping layer thicknesses: H1 (25 nm), H2 (60 nm), H3 (130 nm). (c) Schematic of the upconversion emission measurement setup. (d-f) Energy diagrams showing multiresonant plasmon enhancement in (d) IBR-mediated ASPL, (e) ERS-mediated ASPL, and (f) SHG processes.

In summary, this study marks a significant advancement in dual-modal nanoplasmonic light upconversion. By elucidating the mechanistic differences between ASPL and SHG emissions within broadband multiresonant metal nanocavities, we lay the groundwork for developing multi-modal or wavelength-multiplexed upconversion nanoplasmonic devices. These findings open new avenues in diverse fields such as bioimaging, sensing, interfacial science, nano-thermometry, and integrated photonics, promising enhanced capabilities and broader applications.

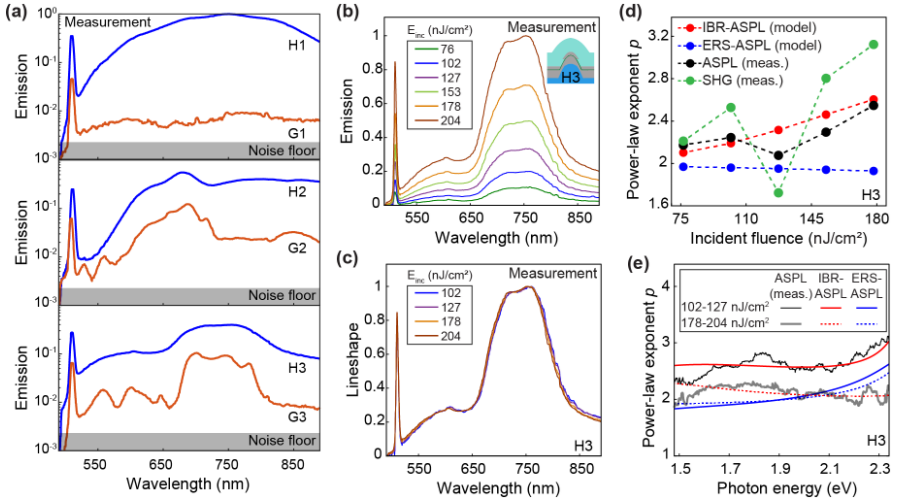

Figure 2: Geometry and Fluence Effects on Upconversion Emission. (a) Upconversion emission spectra of H1/G1, H2/G2, H3/G3 samples under specific ultrashort pulsed laser conditions (P-polarized, λ_{inc}=1020 nm, E_{inc}=204 nJ/cm²). (b-c) Upconversion emission spectra and lineshapes of the H3 sample at different fluence levels (76 to 204 nJ/cm²). (d) Fluence-dependent power-law exponents (p) for SHG and ASPL signals, alongside IBR-ASPL and ERS-ASPL model simulations. (e) Spectrally resolved power-law exponents (p) from ASPL spectra, compared with model simulations across two fluence ranges.

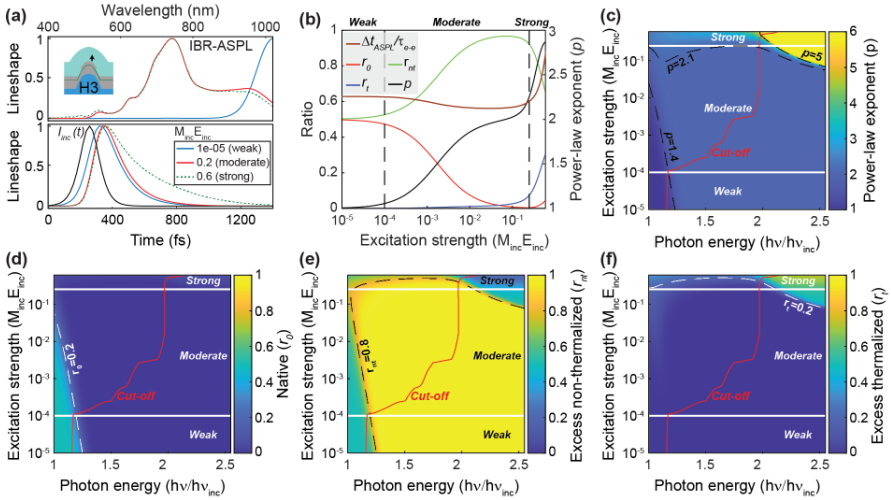

Figure 3: Simulated Excitation Strength Effects on IBR-ASPL Emission. (a) Spectral and temporal lineshapes of ASPL emission at various excitation strengths (weak, moderate, strong) with the temporal lineshape of the incident laser pulse (black curve). (b) Dependence of emission power-law exponent (p), emission duration (Δt_{ASPL}), and carrier contribution ratios (native, excess non-thermalized, excess thermalized) on excitation strength. (c-f) Two-dimensional maps showing dependencies of (c) spectral power-law exponent and (d-f) carrier contribution ratios on emission photon energy and excitation strength, with red line indicating normalized cut-off photon energy of ASPL emission.

2. References

1. Cai, Y.Y., Tauzin, L.J., Ostovar, B., Lee, S. & Link, S. Light emission from plasmonic nanostructures. *J Chem Phys* **155** (2021).
2. Kauranen, M. & Zayats, A.V. Nonlinear plasmonics. *Nature Photonics* **6**, 737-748 (2012).
3. Safiabadi Tali, S.A. et al. Dual-Modal Nanoplasmonic Light Upconversion through Anti-Stokes Photoluminescence and Second-Harmonic Generation from Broadband Multiresonant Metal Nanocavities. *Acs Nano* **17**, 11362-11373 (2023).